Frequency regulation in hybrid power systems using particle swarm optimization and linear matrix inequalities based robust controller design

Shashi Kant Pandey [a], Soumya R. Mohanty [a], Nand Kishor [a], João P.S. Catalão [b,c,d,*]

[a] Motilal Nehru National Institute of Technology, Allahabad 211004, India
[b] University of Beira Interior, R. Fonte do Lameiro, 6201-001 Covilha, Portugal
[c] INESC-ID, R. Alves Redol, 9, 1000-029 Lisbon, Portugal
[d] IST, University of Lisbon, Av. Rovisco Pais, 1, 1049-001 Lisbon, Portugal

ARTICLE INFO

ABSTRACT

It is often necessary to investigate the output power against load demand in a system having distributed generation (DG) resources connected to the existing conventional power system. In this paper, the load frequency control (LFC) problem is presented using different optimization algorithms for two types of power system configurations: (i) hybrid configuration of thermal power system (TPS) integrated with DG, comprising wind turbine generators (WTGs), diesel engine generators (DEGs), fuel cells (FCs), aqua-electrolyzer (AE) and battery energy storage system (BESS); (ii) two area interconnected power system with DG connected in area-1. The inclusion of wind energy system in DG, having high variability in its output power, results into a challenging task for the realization of an effective controller design. This difficulty is further enhanced with random variation of load demand. The control scheme proposed in this paper is based on linear matrix inequalities (LMI) with its parameters tuned by particle swarm optimization (PSO), as a new contribution to earlier studies. The robustness of this controller is thoroughly demonstrated in the above hybrid power systems with different conditions of load disturbances, wind power and parameter variations.

© 2014 Elsevier Ltd. All rights reserved.

Introduction

The installation of distributed generation (DG) resources has being increased to meet the growing energy demand. In general, a DG system makes use of small electric power generation resources located nearby to its consumers and load centers. These generation resources include, among others, wind energy, diesel generator, fuel cells and energy storage systems. To meet the increased load demand of an isolated community, expansion of DG systems may be achieved through interconnection with conventional generation resources. The resulting hybrid power system intends to provide reliable and high quality service to its consumers, and this in turn depends mostly on the type and action of the controller implemented in the system.

Integration of DG resources especially based on wind turbines imposes new challenge to power systems control, making the electric power industry become more complicated.

In such hybrid system, deviations in load demand and stochastic variation in wind power adversely affect the frequency, so it is necessary to preserve the power balance between generation and demand, being achieved through automatic load frequency control (LFC) in some acceptable range. Compliance with frequency regulation policies set by regulation authorities becomes imperative. The frequency control issue in power systems having high penetration of wind systems is addressed in [1–3]. It is important to investigate the impact of high wind power penetration with conventional power flow in the overall area tie-line power. The wind system output power fluctuation dynamics has negative contribution to the power imbalance and thus to the frequency deviation, which should be taken into account in the existing LFC control scheme.

The control scheme implemented seems to be ineffective against wide the range of uncertainties in operation. In fact, frequency deviation in significant range may lead to under/over frequency relay trip and thus disconnection of system loads and generation. The study in this paper is related to the frequency regulation issue in hybrid power systems, with DG resources having negative impact on system frequency profile.

* Corresponding author at: University of Beira Interior, R. Fonte do Lameiro, 6201-001 Covilha, Portugal. Tel.: +351 275 329914; fax: +351 275 329972.
E-mail address: catalao@ubi.pt (J.P.S. Catalão).

Nomenclature

Δf	system frequency deviation (pu Hz)	ΔP_{BESS}	change in BESS power generation (pu MW)
ΔP_{WTG}	change in wind turbine power generation (pu MW)	K_{BESS}	gain constant of BESS
ΔP_{WP}	change in available wind power (pu MW)	T_{BESS}	time constant of the BESS (s)
K_{WTG}	gain constant of the WTG	K_g	governor gain constant
T_{WTG}	time constant of the WTG (s)	T_g	governor time constant (s)
ΔP_{AE}	change in aqua electrolyzer power (pu MW)	T_t	steam turbine constant
K_{AE}	gain constant of the AE	K_r	reheat gain constant
T_{AE}	time constant of the AE (s)	T_r	reheat time constant of the steam turbine
ΔP_{FC}	change in FC power generation (pu MW)	R	drooping characteristic (Hz/pu MW)
K_{FC}	gain constant of the FC	K_p	power system gain (Hz/pu MW)
T_{FC}	time constant of the FC (s)	T_p	power system time constant (s)
ΔP_{DEG}	change in diesel power generation (pu MW)	ΔX_E	small adjustment in position of governor valve (pu MW)
K_{DEG}	gain constant of the diesel generator	ΔP_t	small adjustment in thermal turbine thermal output (pu MW)
T_{DEG}	time constant of the diesel generator (s)		

The different methods to tune gains of PI/PID controllers are given in [4,5]. A linear matrix inequalities (LMI) based linear quadratic regulator (LQR) control design for a wind farm is proposed in [6]. The design of robust PID controller using LMI approach is described in [7]. The application of H_∞ approach in controller design has played an important role in the study of numerous system dynamics since its original formulation. An integration of LMI and static output feedback represents a new approach in the design of PI/PID controllers. The LFC problem using LMI approach with consideration of time delay is also presented by some authors [8–11]. In [8] the authors described the LFC with communication delays using LMI approach. Bevrani and Hiyama [9] proposed a decentralized PI control approach with communication delays being considered as model uncertainty. Design of decentralized robust PI-based LFC for time-delay system is discussed in [10]. Frequency regulation for time-delay power system using LMI approach is described in [11].

The method for PI control design which uses a mixture of H_∞ control and genetic algorithm (GA) method to tune the gains of PI is proposed in [12]. Robust analysis and controller design for LFC is given in [13] and decentralized LFC for multi area power system is given in [14].

In the past, researchers have reported studies on LFC in a conventional system that consists of thermal/hydro or a combination of them using several variants of optimization techniques to design controller gains [15–20]. The performance of such design approach, however, depends not only on the optimization techniques, but also on the objective function. The authors of [18] have used bacteria foraging optimization technique for designing a frequency controller.

The scheme of LFC based on multi-objective GAs is described in [21]. The design of a robust decentralized controller for LFC of multi-area interconnected power systems is discussed in [22,23].

It is worth to mention that in the study considered here, an isolated DG system with conventional power system operates in a local region and is not wide spread over a large geographical region.

Thus, it becomes imperative to perform a study on the hybrid DG system. Further, the uncertainty of intermittent renewable energy resources with generation fluctuation may result in unintentional structure changes, which will further exaggerate the challenge for stabilizing the frequency response.

Recently, some authors [24–29] have reported their study analysing the influence of energy storage in frequency deviation considering renewable resources based DG system. A hybrid power system in an island for frequency control is described in [24]. Small-signal analysis of a hybrid renewable system with energy storage is discussed in [25–27]. The robust H_∞ LFC in hybrid systems is discussed in [28,29].

This paper explores, as a new contribution to earlier studies, the use of particle swarm optimization (PSO) and LMI – PSOLMI based controller design – to achieve minimum frequency deviation. The simulation results are demonstrated on two types of power system configurations. The first one is a hybrid configuration of thermal power system (TPS) integrated with DG, which comprises wind turbine generators (WTGs), diesel engine generators (DEGs), fuel cells (FCs), aqua-electrolyzer (AE) and battery energy storage system (BESS). The second configuration is a two area interconnected power system comprising of DG resources in area-1 with communication delay. The study investigates frequency deviation profile caused by a sudden change in generation and load demand in these two configurations. The robust control scheme via PSOLMI is tested under all possible disturbances, including the intermittent nature of wind speed and other uncertainties.

This paper is organized as follows; the optimization algorithms are given in 'Controller design algorithms', followed by the design strategy for two system configurations in 'Case study-1: hybrid power system' and 'Case study-2: two-area power system with DG', respectively. The simulation results are given in 'Results and discussion on case study-1' and 'Results and discussion on case study-2', and lastly the conclusions are provided in 'Conclusions'.

Controller design algorithms

This section describes an outline of various control designs via LMI approach.

H_∞ control design via LMI approach (H_∞)

The objective of H_∞ control theory is to design the control law u on the basis of measured variable y, so that the effect of disturbance w on control variable z_∞, given in terms of infinity norm of the transfer function from z_∞ to $w, \|T_{z\infty w}\|$ does not surpass a specified limit γ demarcated as assuring robust performance. The classical closed-loop system through H_∞ robust control is represented as Fig. 1, in which $P(s)$ represents a linear-invariant system and $K_\infty(s)$ represents robust H_∞ controller [12].

State space representation of system model is given by:

$$\left. \begin{array}{l} \dot{x} = Ax + B_1 w + B_2 u \\ z_\infty = C_1 x + D_{11} w + D_{12} u \\ y = C_2 x + D_{12} w + D_{22} u \end{array} \right\} \qquad (1)$$

where x is the state variable, w is the disturbance and other exterior input vector, u is the control input, z_∞ and y are controlled and measured output vectors, respectively.
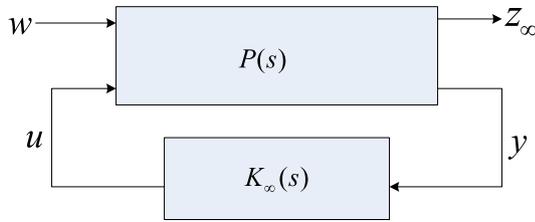
Fig. 1. Closed-loop system via robust H_∞ control.

The state space for controller is considered as:

$$\left.\begin{array}{l} \dot{\xi} = A_k \xi + B_k y \\ u = C_k \xi + D_k y \end{array}\right\} \tag{2}$$

where ξ is the state vector for controller.

From (1) and (2), the subsequent closed loop state-space model is obtained:

$$\left.\begin{array}{l} \dot{x}_{cl} = A_{cl} x_{cl} + B_{cl} w \\ z_\infty = C_{cl} x_{cl} + D_{cl} w \end{array}\right\} \tag{3}$$

where

$$x_{cl} = \begin{bmatrix} x \\ \xi \end{bmatrix} \quad A_{cl} = \begin{bmatrix} A + B_2 C_k C_2 & B_2 C_k \\ B_k C_2 & A_k \end{bmatrix} \quad B_{cl} = \begin{bmatrix} B_1 + B_2 C_k D_{22} \\ B_k D_{22} \end{bmatrix}$$

$$C_{cl} = [C_1 + D_{12} D_k C_2 \quad D_{12} C_k] \quad D_{cl} = [D_{11} + D_{12} D_k D_{22}]$$

Closed-loop root-mean-square (RMS) gain $T_\infty(s)$ or H_∞ norm of transfer function $\|T_{z_\infty w}\|$ does not surpass performance index γ, if and only if there is a symmetric matrix X_∞ such that:

$$\begin{bmatrix} A_{cl} X_\infty + X_\infty A_{cl}^T & B_{cl} & X_\infty C_{cl}^T \\ B_{cl}^T & -I & D_{cl}^T \\ C_{cl} X_\infty & D_{cl} & -\gamma^2 I \end{bmatrix} < 0 \tag{4}$$

$$X_\infty > 0 \tag{5}$$

Therefore, the optimal H_∞ control is attained by the minimization of performance index γ, subject to matrix inequalities (4) and (5).

H_∞ control design for time delay systems

Consider a time-delay system in the subsequent form:

$$\left.\begin{array}{l} \dot{x}(t) = A x(t) + A_d x(t - d) + B_1 w(t) + B_2 u(t) + B_h u(t - h) \\ z_\infty(t) = C_1 x(t) \\ y(t) = C_2 x(t), x(t) \in \psi(t) \quad \forall t \in [-\max(d,h), 0] \end{array}\right\} \tag{6}$$

where h and d denote the delay quantities in input and state, respectively. $\psi(t)$ is a vector-valued continuous initial function. Theorem 1 (given below) adjusts H_∞ model in control synthesis for time-delay systems and creates the conditions for state feedback control law $u(t) = K(t)$ stabilization of (6) and to ensure the H_∞ norm bound γ of closed-loop transfer function $T_{z_\infty w}$, namely $\|T_{z_\infty w}\|_\infty < \gamma; \gamma > 0$.

Theorem 1. State feedback controller K asymptotically studies time-delay system (6) $\|T_{z_\infty w}\|_\infty < \gamma; d, h \geq 0$ and if there occurs symmetric matrices $P > 0$, $Q_1 > 0$, $Q_2 > 0$ fulfilling the LMI

$$\begin{bmatrix} PA_c + A_c^T P + Q_1 + Q_2 & A_d^T P & K^T B_h^T P & C_1 & B_1^T P \\ PA_d & -Q_1 & 0 & 0 & 0 \\ PB_h K & 0 & -Q_2 & 0 & 0 \\ C_1^T & 0 & 0 & I & 0 \\ PB_1 & 0 & 0 & 0 & \gamma^2 I \end{bmatrix} < 0$$

where $A_c = A + B_2 K$.

The LFC problem time-delayed is condensed to the creation of static output feedback (SOF) control $(u(t) = ky(t))$ for time-delay system provided in (6), using Theorem 2. From control law $u(t) = ky(t) = kC_2 x(t)$, and considering Theorem 1, there occurs a memory less feedback control with a constant gain $K = kC_2$. Therefore, $A_c = A + B_2 kC_2$.

Theorem 2. The SOF control asymptotically stabilizes system (6) and $\|T_{z_\infty w}\|_\infty < \gamma; d, h \geq 0$ if there occurs symmetric matrices $Y > 0$, $Q_a > 0$, $Q_b > 0$ satisfying the following LMI:

$$W = \begin{bmatrix} AY + YA^T + Q_a + Q_b & (B_2 kC_2)^T & Y^T & YA_d^T & (B_h kC_2 Y)^T & C_1 Y & B_1^T \\ B_2 kC_2 & -I & 0 & 0 & 0 & 0 & 0 \\ Y & 0 & -I & 0 & 0 & 0 & 0 \\ A_d Y & 0 & 0 & -Q_a & 0 & 0 & 0 \\ B_h kC_2 Y & 0 & 0 & 0 & -Q_b & 0 & 0 \\ YC_1^T & 0 & 0 & 0 & 0 & -I & 0 \\ B_1 & 0 & 0 & 0 & 0 & 0 & -\gamma^2 I \end{bmatrix} < 0$$

In order to define the SOF controller k, the next minimization problem has to be solved:

$$\min_{Q_a, Q_b, Y, k} \gamma \quad \text{subject to} \quad -Y < 0, Q_a < 0, Q_b < 0, W < 0.$$

The proof of Theorem 2 is given in [11].

LMI representation of LQR (LMI-LQR)

Consider a linear time-invariant approach for the proposed power system-1 with the following state space model.

$$\left.\begin{array}{l} \dot{x} = Ax + Bu + \Gamma d \\ y = Cx \\ u = -Ky \end{array}\right\} \tag{7}$$

$$\dot{x} = (A - BKC)x + \Gamma d \tag{8}$$

The variables of the proposed hybrid power system-1 are $x = [\Delta X_E \quad \Delta P_t \quad \Delta P_r \quad \Delta f \quad \Delta P_{WP} \quad \Delta P_{AE} \quad \Delta P_{FC} \quad \Delta P_{DEG} \quad \Delta P_{BESS} \quad \Delta P_{DGS}]^T$ and $y = [\Delta f \quad \Delta P_{DGS}]^T$. The details of LMI representation of LQR are described in [6].

Control design using GALMI approach

The GA is nowadays a popular optimization methodology in many application fields, mostly due to their robust properties in attaining the optimum solution and the capability of reaching a nearly optimal one close to the global minimum solution.

The search mechanism in GA is based on natural selection and persistence of the fittest. The objective function is:

$$\min \gamma = \|T_{z_\infty w}\|_\infty \tag{9}$$

where $\|T_{z_\infty w}\|$ is infinity norm of transfer function from z_∞ to w that does not exceed a specified limit γ.

The robust control design procedure for LFC using GALMI technique is hereafter provided. Consider the state space representation of the system given by:

$$\left.\begin{array}{l} \dot{x} = Ax + B_1 w + B_2 u \\ z_\infty = C_1 x + D_{12} u \\ y = C_2 x \end{array}\right\} \tag{10}$$

The control signal is:

$$u = Ky \tag{11}$$

The chosen controller corresponds to a static output feedback controller, and has inferior complexity than typical H_∞ control design shown in (2). To define the control parameter vector K, from (10) and (11) it can be obtained (12) and (13):

$$u = KC_2x \tag{12}$$

$$\left.\begin{array}{l} \dot{x}_{cl} = A_{cl}x_{cl} + B_{cl}w \\ z_\infty = C_{cl}x_{cl} + D_{cl}w \end{array}\right\} \tag{13}$$

where $A_{cl} = A + B_2KC_2$, $B_{cl} = B_1$, $C_{cl} = C_1 + D_{12}KC_2 D_{cl} = [0]$.

The parameters of the controller specified by K are found with the assistance of GAs for minimizing performance index γ given by (9) determined by the LMIs constraints (4) and (5).

Control design using PSOLMI approach

Particle swarm optimization (PSO) algorithms are population-based evolutionary search techniques with several advantages: they are simple, fast and easy to code. They also require small storage space. PSO approaches are advantageous over GAs. GA is a metaheuristics algorithm based on population size, selection, mutation and crossover, whereas in PSO, with proper choice of parameters and expression of velocity and displacement, the optimization can be more effectively achieved. For instance, each particle in PSO keeps the best local solution as well as the best global solution. The initial population in PSO remains constant and time consuming operators do not exist. If $x_i(t)$ indicates the position of the ith particle in search space at time step t, the new position of the particle is found by adding the velocity component $v_i(t)$:

$$x_i(t+1) = x_i(t) + v_i(t+1) \tag{14}$$

In general, PSO algorithms are grouped in two general categories: the best global solution (gbest), and the best local solution (lbest). In this paper, the gbest algorithm is employed. In gbest PSO algorithm, the vicinity of each particle involves the whole group. In this case, updating the social component of the particle's velocity involves the information acquired from entire particles in the group.

The social information $\hat{y}(t)$ is the best position determined by the swarm. For gbest PSO, particle i velocity is computed by:

$$v_{ij}(t+1) = v_{ij}(t) + c_1r_{1j}(t)[y_{ij}(t) - x_{ij}(t)] + c_2r_{2j}(t)[\hat{y}_j(t) - x_{ij}(t)] \tag{15}$$

where $v_{ij}(t)$ indicates the velocity of particle i at dimension $j = 1, 2, \ldots, n_x$ at time step t, $x_{ij}(t)$ is the position of particle i at dimension j, c_1 and c_2 are acceleration factors and $r_{1j}(t)$ and $r_{2j}(t)$ are random variables with normal distribution in [0,1]. The last two variables incorporate randomness in the algorithm.

The proposed PSOLMI design uses PSO procedure to find the optimum values for PI controller, considering the H_∞ constraints in terms of LMIs in (4) and (5). This brings about the robust performance of H_∞ control for PI controller and makes system vulnerable against bounded uncertainties. The problem formulation for PSOLMI is the same as GALMI, as discussed previously.

Case study-1: hybrid power system

The LFC study being limited to small perturbations, the system models are usually adequately represented by a linearized one. The interconnected conventional reheated thermal source along with DG resources forming a hybrid power system is provided in Fig. 2.

The DG system under study consists of energy resources such as WTG, FC, AE, DEG, and BESS. The dynamic behavior of a power system in the presence of wind power generation systems might

be different from conventional power plants. The power outputs of such sources are depending on weather conditions seasons and geographical location. When wind power is a part of the power system, additional imbalance is created when the actual wind power deviates from its forecast due to wind speed variations. So, scheduling conventional generators units to follow load (based on the forecasts) may also be affected by wind power. Because wind power is an intermittent source which differs from the traditional plants, the control of wind turbine output is much more challenging. When demand is beyond the limit of available wind power, stability problems may arise. Therefore, an appropriate coordination between stability and controllability of active power in wind turbines should be further defined. A part of wind power generator output is utilized by AE for hydrogen production, which is used in FC to generate power. The BESS is used in the power system to perform the function of load levelling. The mathematical models of the different subsystems in the DG power system are presented as follows [25–27]:

Wind power turbine

The power of the wind turbine generator depends upon the wind speed. Wind speed varies continuously with time. The mechanical power output of the wind turbine is proportional to the cube of wind speed. The wind power is given as:

$$P_{WP} = \frac{1}{2}\rho A_R C_P V_W^3 \tag{16}$$

where ρ: the air density (kg/m^3); A_R: the swept area of blade (m^2) and C_P: Power coefficient, a function of tip speed ratio (λ) and blade pitch angle (β), V_W: wind speed. The wind turbine system has several nonlinearities. When wind turbine uses its pitch controller to counteract utility grid frequency oscillations, its output power varies. Hence, the pitch angle set point is a nonlinearity limited by the boundaries of variation in output power. The pitch system, which is used to turn the pitch angle according to wind speed, introduces nonlinearity. The transfer function of wind turbine generator is given by first-order lag neglecting nonlinearities:

$$G_{WTG}(s) = \frac{\Delta P_{WTG}}{\Delta P_{WP}} = \frac{K_{WTG}}{1 + sT_{WTG}} \tag{17}$$

Aqua-electrolyzer for hydrogen production

A part of the wind power generator output is utilized by aqua electrolyzer for hydrogen production, which is used in the fuel cell to generate power. The transfer function of the AE can be expressed by first-order lag as:

$$G_{AE}(s) = \frac{\Delta P_{AE}}{u_2} = \frac{K_{AE}}{1 + sT_{AE}} \tag{18}$$

Fuel cell power generation

The FC is an electrochemical device, which converts the chemical energy of fuel (hydrogen) into electrical energy by combining gaseous hydrogen with air in the absence of combustion. They are considered to be an important resource in hybrid distributed power systems due to several advantages, such as high efficiency and low pollution. FC generator is a higher order model and has non linearity. For low frequency domain analysis, it is represented by a first order lag transfer function as:

$$G_{FC}(s) = \frac{\Delta P_{FC}}{u_2} = \frac{K_{FC}}{1 + sT_{FC}} \tag{19}$$
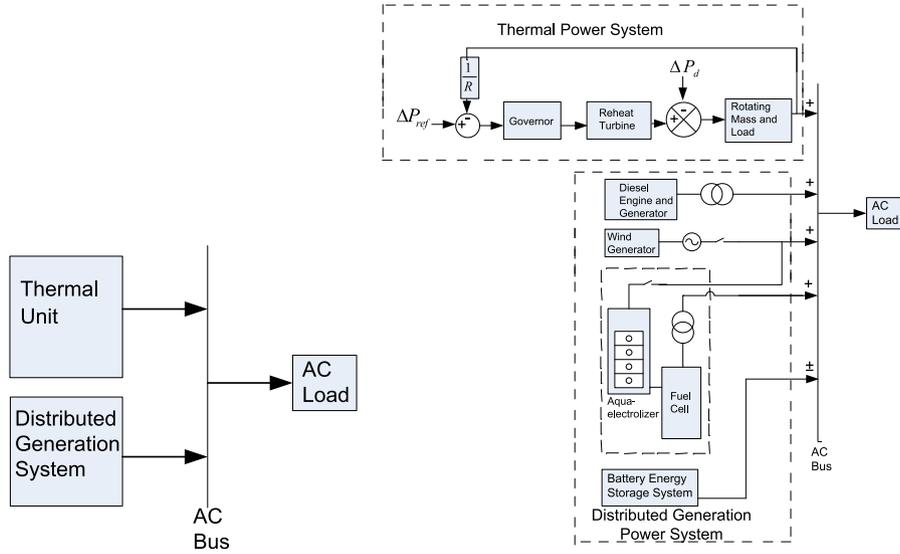
(a) Block diagram
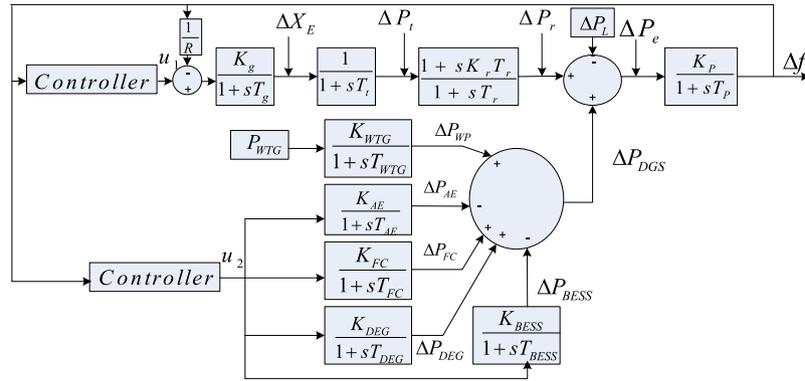
(b) Transfer function model

Fig. 2. Case study-1: hybrid power system configuration.

Diesel engine power generation

The DEG is in action autonomously to supply the deficit power in the hybrid DG system to meet the supply-load demand balance condition. A diesel generator is a nonlinear system because of the presence of a nonlinear, time-varying dead time between the injection and production of mechanical torque. The transfer function of DEG can be given by linear first order lag as:

$$G_{DEG}(s) = \frac{\Delta P_{DEG}}{u_2} = \frac{K_{DEG}}{1 + sT_{DEG}} \tag{20}$$

Battery energy storage system

The BESS is used to provide additional damping to power system swings to improve both transient and dynamic stability. The wind power has an intermittent nature, and short time power fluctuation may cause large problems for power systems operation. A possible solution is use of energy storage devices.

The BESS is very affective to store large amount of wind power due to its very good technical characteristics, like large energy density and fast access time. The transfer function of the BESS can be first order lag given as:

$$G_{BESS}(s) = \frac{\Delta P_{BESS}}{u_2} = \frac{K_{BESS}}{1 + sT_{BESS}} \tag{21}$$

The power-frequency balance is achieved by control signals u_1 and u_2 fed from the designed controller. The details of mathematical models of different modules in the hybrid DG power system are described in [25–27], as well as the data of different components in the DG power system under study.

Power balance is attained by the following equation:

$$\Delta P_e = \Delta P_{DGS} + \Delta P_{TH} - \Delta P_L \tag{22}$$

where ΔP_e is the error in power supply, ΔP_{DGS} is the output power of DG system, $\Delta P_{TH}(=\Delta P_r)$ is the output power of reheat thermal system and ΔP_L is the change in load demand.

The total output power of the hybrid DG system is expressed by:

$$\Delta P_{DGS} = \Delta P_{WP} + \Delta P_{FC} - \Delta P_{AE} + \Delta P_{DEG} \pm \Delta P_{BESS} \tag{23}$$

where ΔP_{WP}, ΔP_{FC}, ΔP_{AE}, ΔP_{DEG}, ΔP_{BESS} are the power generation by the WTG, FC, AE, DEG and BESS, respectively. The impact of wind power variation on system frequency response is a key factor to analyse the LFC issue in hybrid systems comprising DG resources.

The deviation in the frequency outline Δf is given by $\Delta f = \frac{\Delta P_e}{K_{sys}}$, where K_{sys} is the system frequency characteristic constant.

The transfer function for system frequency variation to pu deviation in power is given by:

$$T_{sys} = \frac{\Delta f}{\Delta P_e} = \frac{1}{K_{sys}(1 + sT_{sys})} = \frac{K_P}{1 + sT_P} \tag{24}$$

where K_P and T_P are the equivalent gain constant and time constant, respectively.

In steady state condition, the power generation is matched with load demand, driving the frequency deviation to zero. The balance between power generation and load demand is achieved by virtue of change in frequency to generate the control signal through the controller, as shown in Fig. 2(b). The input exogenous signals w_1 and w_2 are the load disturbance and wind power variation, respectively, i.e.

$$and \quad \left. \begin{array}{l} w_1 = \Delta P_L \\ w_2 = \Delta P_{WTG} \end{array} \right\} \tag{25}$$

Now, consider the state space model as (10) with following state:

$$x = \begin{bmatrix} \Delta X_E & \Delta P_t & \Delta P_r & \Delta f & \Delta P_{WP} & \Delta P_{AE} & \Delta P_{FC} \\ \Delta P_{DEG} & \Delta P_{BESS} & \Delta P_{DGS} & \int \Delta f \end{bmatrix}^T$$

$$w = [\, w_1 \quad w_2 \,]^T, u = [\, u_1 \quad u_2 \,]^T, \quad y = [\, \Delta f \quad \int \Delta f \,]^T$$

Robust controller K is capable of minimizing the fictitious output z_∞ in the occurrence of w. Thus, the vector z_∞ should adequately cover all signals that are to be minimized to achieve the desired response. Therefore, a suitable fictitious output vector may be chosen as:

$$z_\infty = [\, \eta_1 \Delta f \quad \eta_2 \int \Delta f \quad \eta_3 u_1 \quad \eta_4 u_2 \,]^T \tag{26}$$

where $\eta_i (i = 1, 2 \ldots 4)$ are constraint weighting coefficients and should be selected by the designer to achieve the preferred performance.

The control signal for the proposed power system-1 is written as:

$$u = K_p \Delta f + K_i \int \Delta f = \begin{bmatrix} u_1 \\ u_2 \end{bmatrix} \begin{bmatrix} K_{p1} & K_{i1} \\ K_{p2} & K_{i2} \end{bmatrix} \begin{bmatrix} \Delta f \\ \int \Delta f \end{bmatrix} = Ky \tag{27}$$

The controller sends a command signal to the conventional power system (thermal) and DEGs, FCs, AE and BESS in order to regulate the active power and thereby regulate the system frequency. In order to define the control parameter vector K, the closed-loop system is obtained as (13).

Case study-2: two-area power system with DG

The conventional framework of the power system is modified with the incorporation of thermal and DG in area-1 and thermal power in area-2, respectively. The block diagram of the proposed structure is shown in Fig. 3(a) and its transfer function model is presented in Fig. 3(b).

The LFC model in traditional structure with time delays is discussed in [8,10]. In interconnected 2-area power systems the communication delay comes into play, which affects the controller performance. In view of this, in the control input and output in each area of the LFC structure, the communication delays are depicted as shown in Fig. 3(b). An exponential function $e^{-\tau s}$ is used to describe the communication delay, where τ represents the communication delay time. To generate the area control error (ACE) signal, the detected frequency and tie-line power deviations via communication line is used.

The plant state space model is developed as:

$$x = \begin{bmatrix} \Delta X_{E1} & \Delta P_{t1} & \Delta P_{r1} & \Delta f_1 & \Delta X_{E2} & \Delta P_{t2} & \Delta P_{r2} \\ \Delta f_2 & \Delta P_{TIE} & \Delta P_{WP} & \Delta P_{AE} & \Delta P_{FC} & \Delta P_{DEG} & \Delta P_{BESS} \\ \int ACE_1 & \int ACE_2 \end{bmatrix}^T$$

$$y = [\, ACE_1 \quad \int ACE_1 \quad ACE_2 \quad \int ACE_2 \,]^T$$

$$w = [\, \Delta P_{L1} \quad \Delta P_{L1} \quad \Delta P_{WTG} \,]^T$$

$$u = [\, u_1 \quad u_2 \quad u_3 \,]^T$$

$$z_\infty = [\, \eta_1 \Delta f_1 \quad \eta_2 \Delta f_2 \quad \eta_3 \Delta P_{TIE} \quad \eta_4 u_1 \quad \eta_5 u_2 \quad \eta_6 u_3 \,]^T$$

where $\eta_i (i = 1, 2 \ldots 6)$ are constraint weighting coefficients and should be chosen by the designer to achieve the wanted performance. The ACE signal in multi-area LFC structure is given by:

$$ACE_i = \beta_i \Delta f_i + \Delta P_{TIEi} \tag{28}$$

where ΔP_{TIEi} is the net exchange of tie-line power of control ith area. The control signal is written as:

$$u = K_p ACE + K_i \int ACE = \begin{bmatrix} u_1 \\ u_2 \\ u_3 \end{bmatrix} = \begin{bmatrix} K_{p1} & K_{i1} & 0 & 0 \\ K_{p2} & K_{i2} & 0 & 0 \\ 0 & 0 & K_{p3} & K_{i3} \end{bmatrix} \begin{bmatrix} ACE_1 \\ \int ACE_1 \\ ACE_2 \\ \int ACE_2 \end{bmatrix} = ky \tag{29}$$

Results and discussion on case study-1

This section discusses the simulation analysis with the above described controllers in hybrid DG power system. The LFC scheme in an interconnected hybrid power system should control the area frequency as well as the tie-line power flow between the control areas.

- *Load demand change*

The controller response is tested for step load and random load change.

Step load change: The load disturbance and wind power variation applied to the hybrid DG system are considered as $\Delta P_L = 0.01$ pu and $\Delta P_{WTG} = 0.01$ pu. The frequency deviation profile (Δf) for various controllers is presented in Fig. 4. With the PSOLMI, the frequency deviation of the system is quickly damped with comparatively reduced undershoot. The frequency deviation takes about 10 s to settle down to the steady-state.

Random step load change: The load disturbance variation in steps as shown in Fig. 5(a) with $\Delta P_{WTG} = 0.01$ pu is applied to the system. The system frequency deviation is provided in Fig. 5(b). It is observed that PSOLMI controller achieves comparatively better damping for frequency deviation profile. The control effort of the proposed PSOLMI is improved comparatively to the other controllers in terms of low overshoot/undershoot and faster settling time.

Random load change: The random load variation as shown in Fig. 6(a) and $\Delta P_{WTG} = 0.01$ pu is applied to the system. System response to frequency deviation is shown in Fig. 6(b). The PSOLMI controller performance remains consistent as discussed previously. The response is characterized by low overshoot/undershoot, less oscillation and faster response.

Both GA and PSO are similar in the sense that these two techniques are population-based search methods and they search for the optimal solution by updating generations. Since the two approaches are supposed to find a solution to a given objective function but employ different strategies and computational effort, it is appropriate to compare their performance. It should be noted that while the GA is inherently discrete, i.e. it encodes the design variables into bits of 0's and 1's, therefore it easily handles discrete design variables, PSO is inherently continuous and must be modified to handle discrete design variables. Compared with GA, PSO has some attractive characteristics. It has memory, so knowledge of good solutions is retained by all particles; whereas in GA,

(a) Block diagram

(b) Transfer function
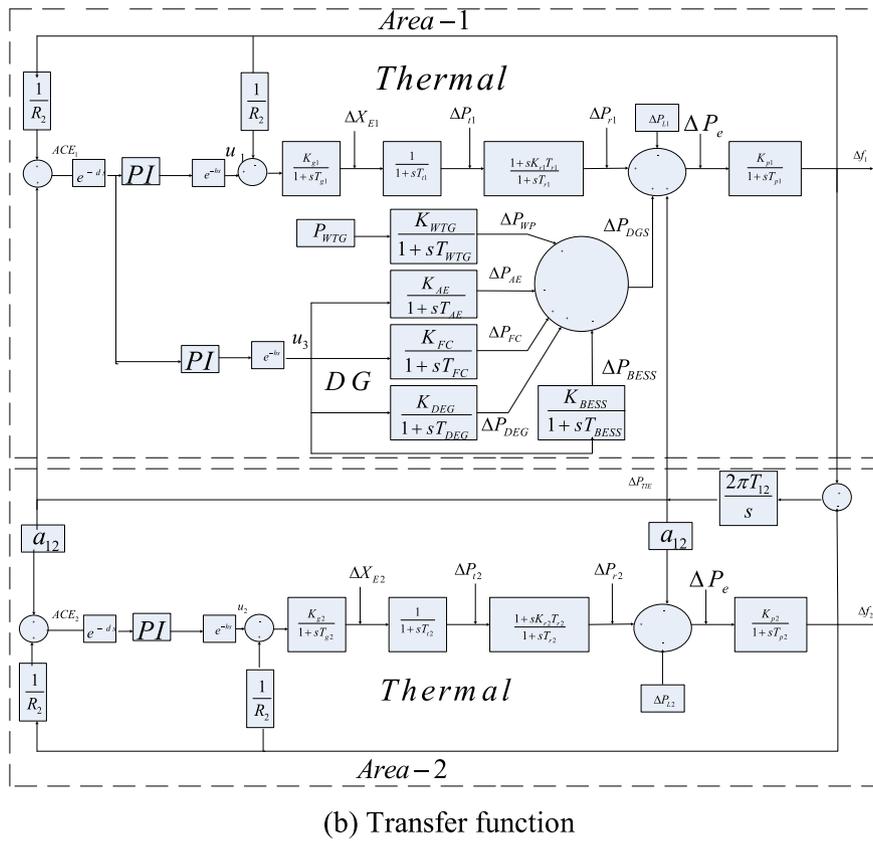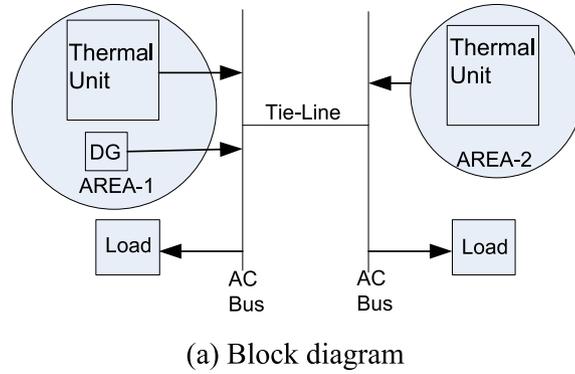
**Fig. 3.** Case study-2: two area power system with DG.
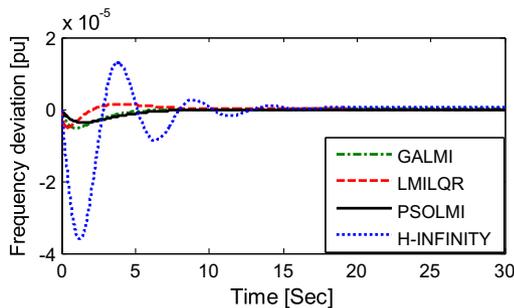
Fig. 4. Response with step load change.

previous knowledge of the problem is destroyed once the population changes. PSO has constructive cooperation between particles, so particles in the swarm share information between them.

The response with PSOLMI is much faster, with less overshoot and settling time compared to GALMI and LMILQR. The PSOLMI controller has good damping characteristics to low frequency oscillations and stabilizes the system much faster. This extends the power system stability limit and the power transfer capability.

• *Input wind power change*

Step change in wind power input: The random step change in wind power input as shown in Fig. 7(a) is applied to the system with $\Delta P_L = 0.01$ pu. The variation in system frequency deviation is presented in Fig. 7(b). The response achieved by PSOLMI controller is again better (low overshoot/undershoot and fast settling time) than other controllers.

Random wind power input: The random wind power input as shown in Fig. 8(a) with $\Delta P_L = 0.01$ pu is applied to the system. Fig. 8(b) shows the corresponding system frequency deviation. With the proposed PSOLMI controller, the oscillation of frequency

(a) Load change pattern

(b) Frequency deviation
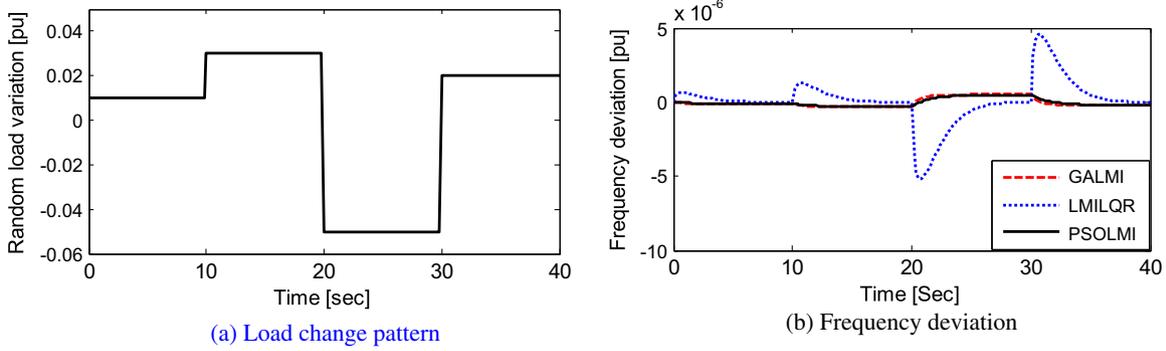
Fig. 5. Response with random step load change.

(a) Random load variation

(b) Frequency deviation
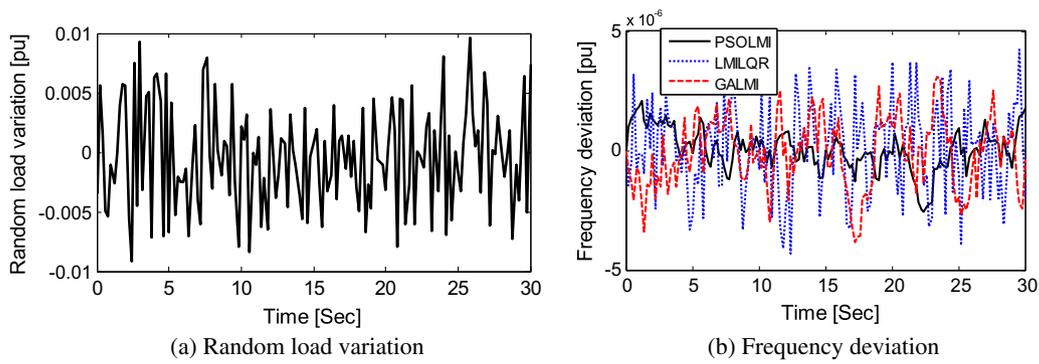
Fig. 6. Response with random load variation.

(a) Step change in wind power

(b) Frequency deviation
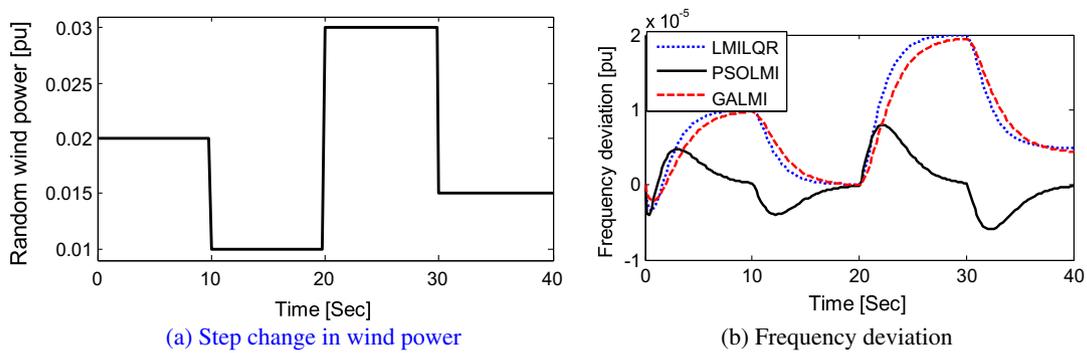
Fig. 7. Response for case study-1 with step change in wind power.

(a) Random wind power variation

(b) Frequency deviation
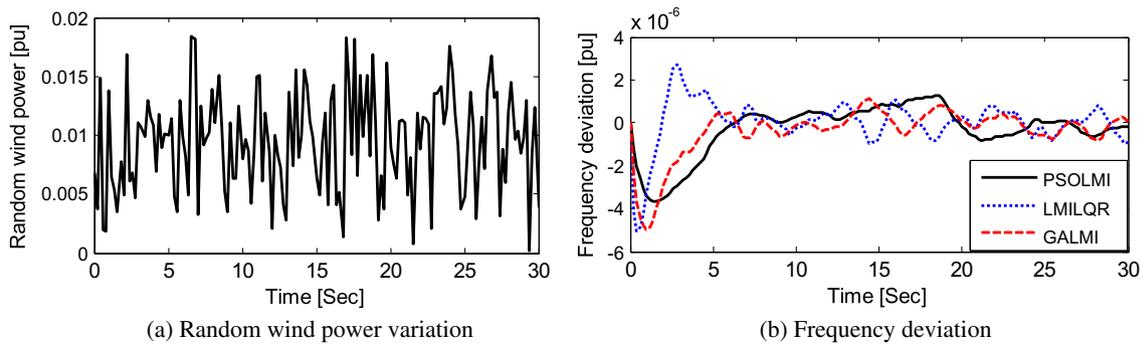
Fig. 8. Response with random wind power variation.
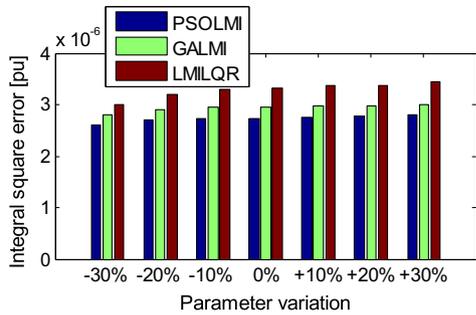
Fig. 9. Computed ISE for uncertainties in all system parameters.

• *Parameter variations*

Any controller designed for fixed plant parameter or tuned to nominal conditions may not perform satisfactory with changes in their nominal values. Also, in some cases, the value of these parameters is not accurately determined, either experimentally or mathematically. So, a controller design is desired to be robust enough against uncertainties in parameter values of the system model. The robustness of the controllers is evaluated by computation of a quantitative performance index, the integral square error (ISE) index given as:

$$\text{ISE} = \int_0^{30} (\Delta f)^2 dt \qquad (30)$$

deviation is significantly diminished, suggesting robust performance of the proposed controller against stochastic variations of wind power due to weather conditions as input disturbance.

The computed values of ISE for the various controllers are depicted in Fig. 9. As observed for the change in parameters in the range of +30% to −30% from nominal value, the corresponding value
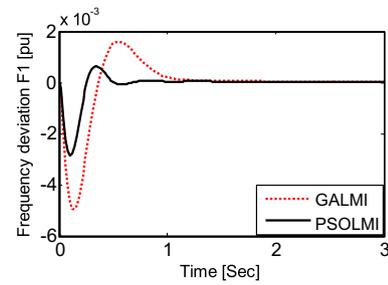
(a) Frequency deviation in area-1
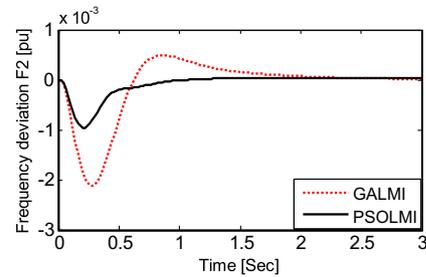
(b) Frequency deviation in area-2
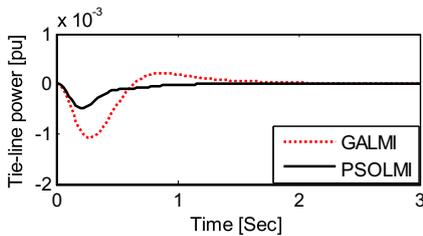
(c) Tie-line power deviation
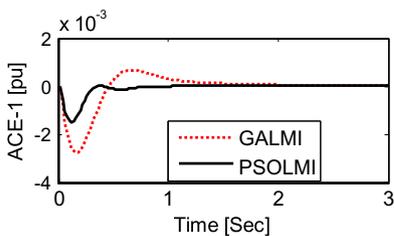
(d) ACE in area-1
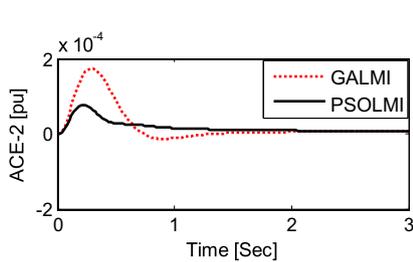
(e) ACE in area-2
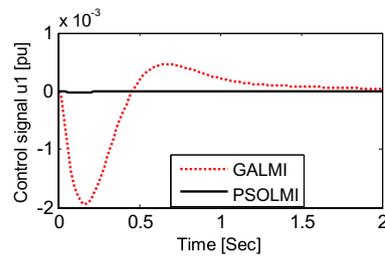
(f) Control signal u$_1$
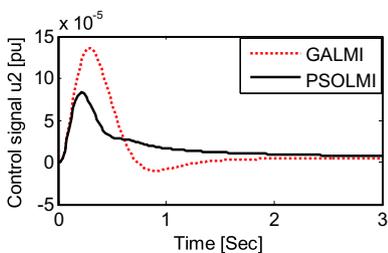
(g) Control signal u$_2$
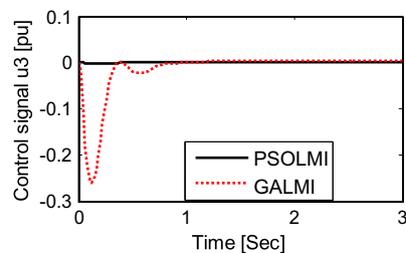
(h) Control signal u$_3$

Fig. 10. Response for case study-2 with step load change.

(a) Frequency deviation in area-1

(b) Frequency deviation inarea-2

(c) Tie-line power deviation
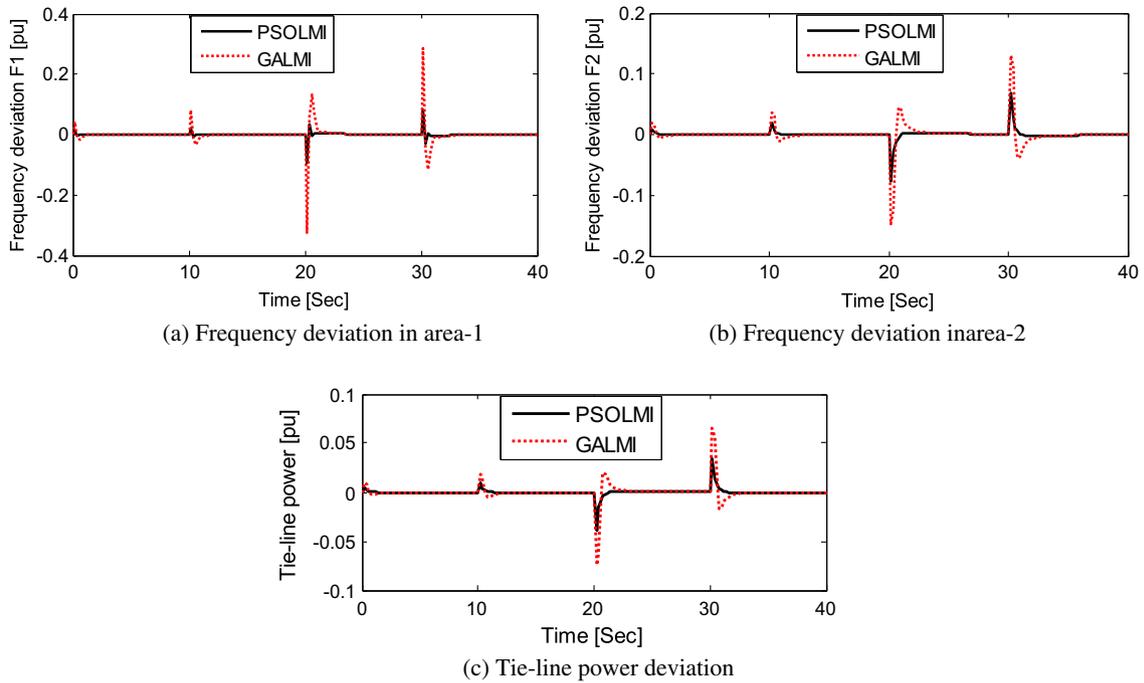
Fig. 11. Response for case study-2 with random step load change.

(a) Frequency deviation in area-1

(b) Frequency deviation in area-2


(c) Tie-line power deviation
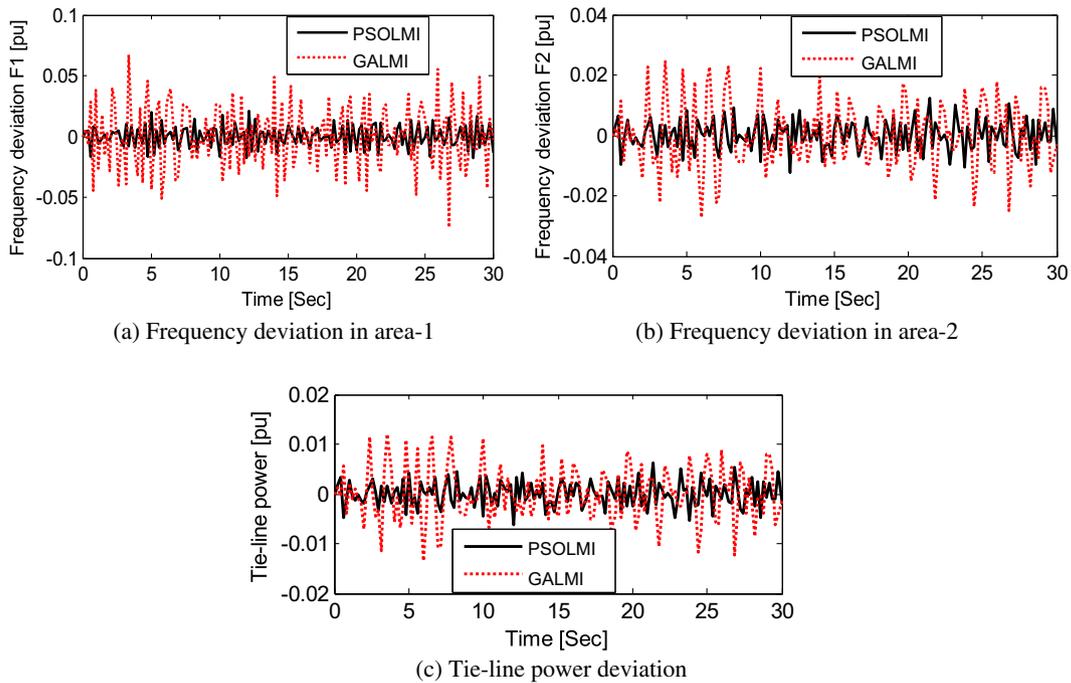
Fig. 12. Response for case study-2 with random load variation.

of index is computed to be higher for LMI-LQR and GALMI, compared to PSOLMI controller. Also, it is evident that a consistent value of the index is obtained. These results successfully validate that the proposed controller not only compensates against parameters variations but also regulates the frequency deviation profile adequately. It is found that robustness is guaranteed under both upper bound (+30%) and lower bound (−30%) of parameter changes.

Results and discussion on case study-2

This section discusses the simulation analysis conducted on case study-2 using different optimization algorithms. It becomes imperative to investigate the response variation, when existing thermal with DG resources (area 1) are interconnected to another thermal system (area 2).

(a) Frequency deviation in area -1

(b) Frequency deviation in area -2

(c) Tie-line power deviation
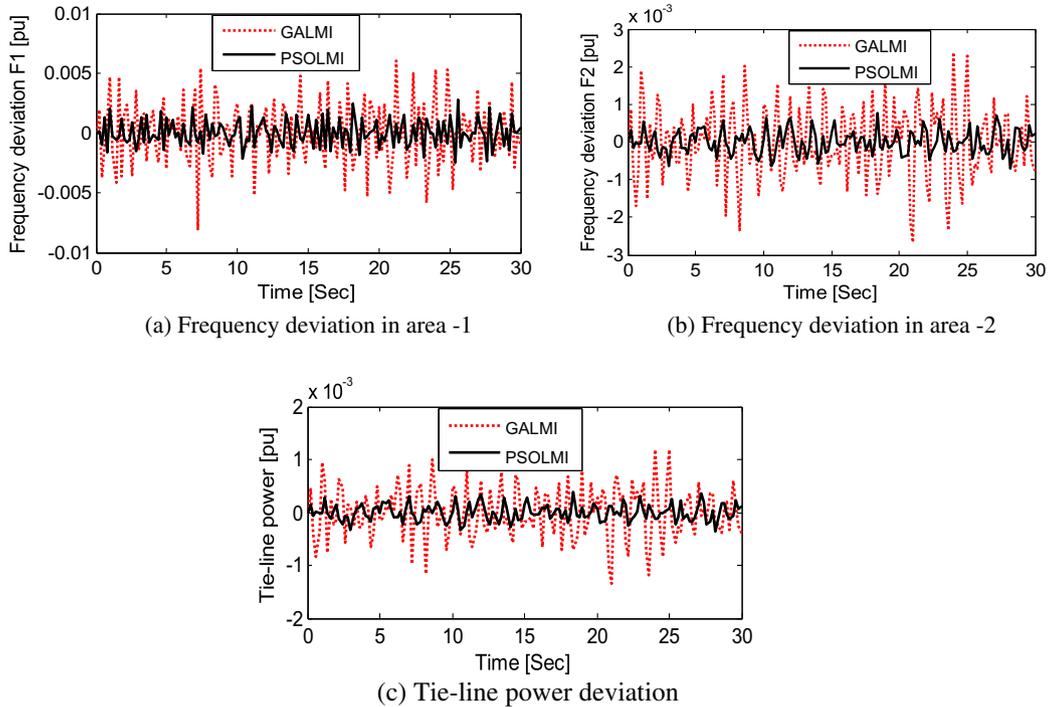
Fig. 13. Response for case study-2 with random wind power variation.

Load demand change

The response of the controllers is tested for step load and random load change.

Step load change: The load disturbance and wind power variation applied to the power system-2 is considered as ΔP_{L1} = 0.01 pu, ΔP_{L2} = 0.01 pu and ΔP_{WTG} = 0.01 pu. The responses obtained are shown in Fig. 10.

Fig. 10(a) and (b) represent the frequency deviation in areas 1 and 2, respectively. The frequency deviation takes about 1.0 s to reach steady-state. The tie-line power deviation is shown in Fig. 10(c). Fig. 10(d) and (e) represent the ACE in area-1 and area-2, respectively. By using the proposed method, PSOLMI, the frequency deviation of the system is quickly damped with comparatively reduced undershoot.

The time-domain characteristics (undershoot and settling time of frequency deviation) using PSOLMI controller is lower than those obtained by GALMI controller. The peak frequency deviation remains low and has reduced significantly in shorter time period in case of PSOLMI controller. Fig. 10(f), (g) and (h) represent the control signals. The control effort required by PSOLMI controller is low and also for short time span.

Random step load change: Consider the load disturbance being varied in steps as shown in Fig. 5(a) in area-1 with ΔP_{L2} = 0.01 pu and ΔP_{WTG} = 0.01 pu applied to the system. The system responses are illustrated in Fig. 11(a)–(c). It is observed that PSOLMI controller achieves comparatively better damping for frequency deviation profile and optimal tie-line power changes. Thus, the obtained results illustrate better performance despite load disturbances. Further, comparison of Fig. 5 (case study-1) and Fig. 11 (case study-2), a smaller settling time, but an increased overshoot/undershoot in the dynamics of frequency deviation is observed in latter system under the same load disturbance. This is due to the fact that, during the load disturbance, the tie line supports the control area by absorbing power.

Random load variation: The random load variation as shown in Fig. 6(a) in area-1 with ΔP_{L2} = 0.01 pu and ΔP_{WTG} = 0.01 pu is considered. The frequencies and tie-line power deviations are shown in Fig. 12(a)–(c). The PSOLMI controller performance suggests a general trend, i.e. remains consistent as discussed previously. The response is characterized by low overshoot/undershoot, less oscillation and faster response. The control scheme provides smooth performance under transient characteristic of disturbances. On the other hand, as compared to Fig. 6(b), the frequency deviation dynamics is accompanied by higher amplitudes and oscillation about the steady state value.

Input wind power change

Consider the load disturbance, ΔP_{L1} = 0.01 pu, ΔP_{L2} = 0.01 pu and random wind power input applied to the system. The frequency and tie-line power deviation profiles are shown in Fig. 13. The proposed controller PSOLMI performs satisfactorily, minimizing the frequency deviation in area 1, having strong interactions with area 2. These results indicate improved performance accommodating the wind power uncertainty. A close observation suggests comparatively higher frequency deviation in area 1 with respect to area 2.

The change in wind power generation, change in AE power generation, change in FC power generation, change in diesel power generation, change in BESS power generation, change in total DG power generation, change in power generation in area-1 and change in power generation in area-1 for load disturbance and wind power variation of ΔP_{L1} = 0.01 pu, ΔP_{L2} = 0.01 pu, and ΔP_{WTG} = 0.01 pu are all shown in Fig. 14(a)–(h), respectively.

Effect of communication delays

The effect of communication time delay on the behaviour of the power system for GALMI controller is shown in Fig. 15(a)–(c). Although the communication delay influences the controller performance, as discussed earlier, with PSOLMI the controller performance is almost insensitive to the effect of communication delay, as shown in Fig. 15(d) and (f).
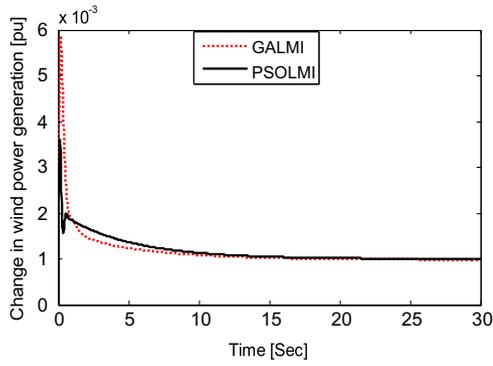
(a) Change in wind power generation
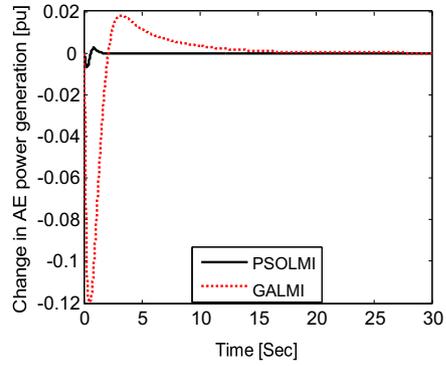
(b) Change in AE power generation
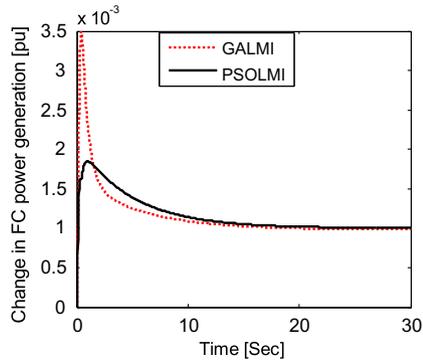
(c) Change in FC power generation
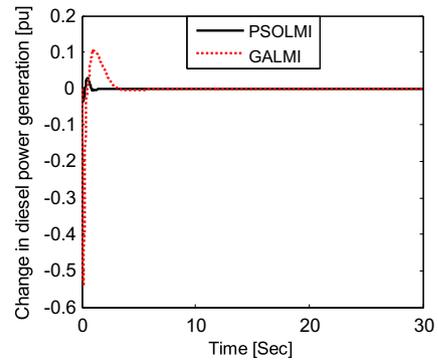
(d) Change in diesel power generation
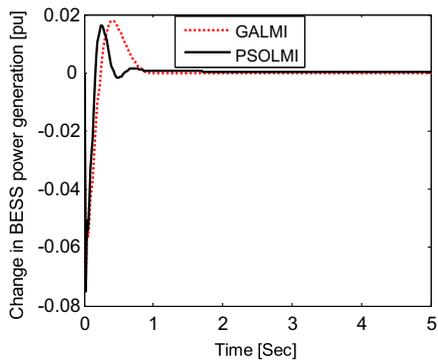
(e) Change in BESS power generation
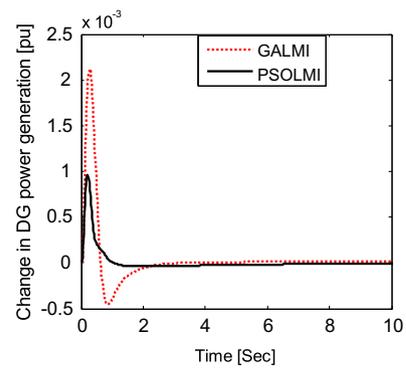
(f) Change in total DG power generation
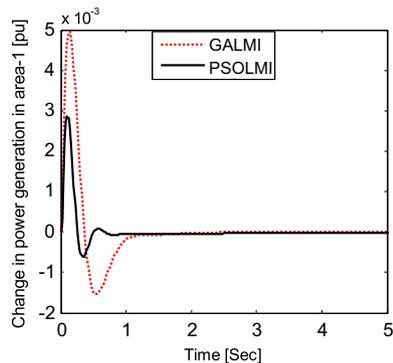
(g) Change in power generation in area-1
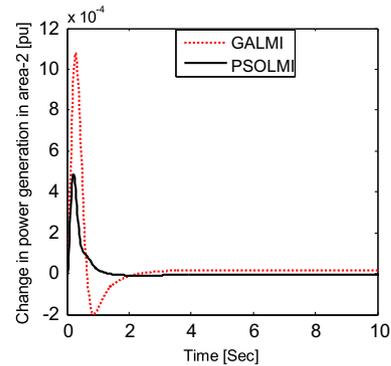
(h) Change in power generation in area-2

Fig. 14. Response of change in power generation for case study-2 with step load change.

(a) Frequency deviation in area-1

(b) Frequency deviation in area-2

(c) Tie-line power deviation

(d) Frequency deviation in area-1

(e) Frequency deviation in area-2

(f) Tie-line power deviation
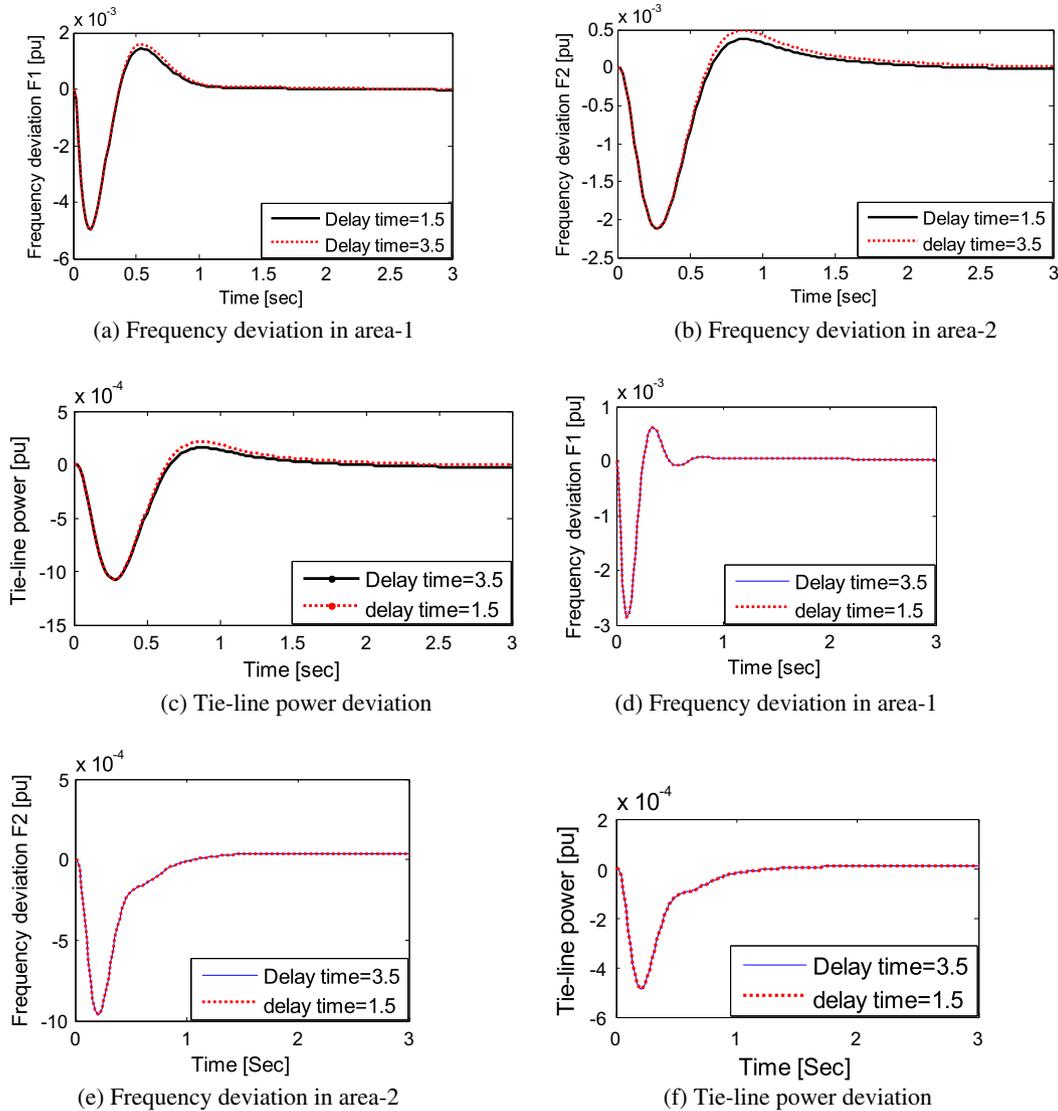
Fig. 15. Response for case study-2 with time delays.

Robustness with parameter variations

The robustness of the controllers is evaluated by the computation of integral square error (ISE) for changes in parameters given as:

$$\text{ISE} = \int_0^{30} \left(\Delta f_1^2 + \Delta f_2^2 + \Delta P_{TIE}^2 \right) dt \qquad (31)$$

The values of ISE are shown in Fig. 16. As observed for the change in parameters over a large percentage range with respect to nominal value, the corresponding indices are higher in case of GALMI as compared to PSOLMI controller.

These results successfully validate that the proposed controller not only compensates against parameters variations but also regulates the frequency deviation profile adequately.

Thus, for the LFC problem, PSO is superior to GA due to its simplicity, better convergence and computational time. This is the reason of improvement. Both GA and PSO are similar in the sense that these two techniques are population-based search methods and they search for the optimal solution by updating generations. Since the two approaches are supposed to find a solution to a given objective function but employ different strategies and computational effort, it is appropriate to compare their performance. It
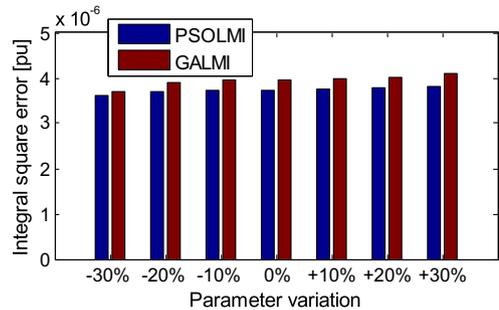

Fig. 16. Computed ISE for change in all system parameters.

should be noted that while the GA is inherently discrete, i.e. it encodes the design variables into bits of 0's and 1's, therefore it easily handles discrete design variables, PSO is inherently continuous and must be modified to handle discrete design variables. Compared with GA, PSO has some attractive characteristics. It has memory, so knowledge of good solutions is retained by all particles; whereas in GA previous knowledge of the problem is destroyed once the population changes. PSO has constructive cooperation between particles, so particles in the swarm share information between them.

S.K. Pandey et al. / Electrical Power and Energy Systems 63 (2014) 887–900

Conclusions

In this paper, the LFC problem was presented using several control algorithms for the power system consisting of different energy sources. The new contribution of this research was the successful simulation of the proposed PSOLMI controller, demonstrating superior performance as compared to other controllers. The results illustrated superior control effort and guaranteed robust performance as compared to H_∞, LMI-LQR and GALMI controllers, against various uncertainties such as wind power variation and load change. The PSOLMI controller effectiveness on minimizing frequency deviation was validated for a variation in the parameters of about ±30% from nominal value. Hence, it was shown that PSOLMI controller has adequate disturbance rejection properties and thereby robustness in its performance. This improves system reliability, minimizing grid frequency oscillation and enhancing closed loop stability. Further, the comparison of the dynamics of case studies 1 and 2 suggested increased amplitude and oscillation of frequency deviation profiles in case of existing thermal with DG resources that are interconnected to another thermal system.

Acknowledgements

References

[1] Li Hui, Liu Shengquan, Ji Haiting, Yang Dong, Yang Chao, Chen Hongwen, et al. Damping control strategies of inter-area low-frequency oscillation for DFIG-based wind farms integrated into a power system. Int J Electr Power Energy Syst 2014;61:279–87.

[2] Howlader Abdul Motin, Izumi Yuya, Uehara Akie, Urasaki Naomitsu, Senjyu Tomonobu, Saber Ahmed Yousuf. A robust H-infinity controller based frequency control approach using the wind-battery coordination strategy in a small power system. Int J Electr Power Energy Syst 2014;58:190–8.

[3] Li Yujun, Zhang Zeren, Yang Yong, Li Yingyi, Chen Hairong, Xu Zheng. Coordinated control of wind farm and VSC–HVDC system using capacitor energy and kinetic energy to improve inertia level of power systems. Int J Electr Power Energy Syst 2014;59:79–92.

[4] Ali ES, Abd-Elazim SM. BFOA based design of PID controller for two area load frequency control with nonlinearities. Int J Electr Power Energy Syst 2013;51:224–31.

[5] Debbarma Sanjoy, Saikia Lalit Chandra, Sinha Nidul. Automatic generation control using two degree of freedom fractional order PID controller. Int J Electr Power Energy Syst 2014;58:120–9.

[6] Hee-Sang Ko, Juri Jatskevich, Guy Dumont, Gi-Gap Yoon. An advanced LMI-based-LQR design for voltage control of grid-connected wind farm. Electr Power Syst Res 2008;78:539–46.

[7] Ge Ming, Chiu Min-Sen, Wang QG. Robust PID controller design via LMI approach. J Process Control 2002;12:3–12.

[8] Yu Xiaofeng, Tomsovic K. Application of linear matrix inequalities for load frequency control with communication delays. IEEE Trans Power Syst 2004;19(3):1508–15.

[9] Bevrani H, Hiyama T. On load-frequency regulation with time delays: design and real-time implementation. IEEE Trans Energy Convers 2009;24(1):292–300.

[10] Bevrani H, Hiyama T. Robust decentralized PI based LFC design for time delay power systems. Energy Convers Manage 2008;49:193–204.

[11] Bevrani H. Robust power system frequency control. Power electronics and power systems. Springer; 2008.

[12] Rerkpreedapong D, Hasanovic A, Feliachi A. Robust load frequency control using genetic algorithms and linear matrix inequalities. IEEE Trans Power Syst 2003;18(2):855–61.

[13] Tan Wen, Zhan Xu. Robust analysis and design of load frequency controller for power systems. Electr Power Syst Res 2009;79:846–53.

[14] Alrifai MT, Hassan MF, Zribi M. Decentralized load frequency controller for a multi-area interconnected power system. Int J Electr Power Energy Syst 2011;33:198–209.

[15] Ghosal SP. Optimization of PID gains by particle swarm optimization in fuzzy based automatic generation control. Electr Power Syst Res 2004;72:203–12.

[16] Ahamed TPI, Rao PSN, Sastry PS. A reinforcement learning approach to automatic generation control. Electr Power Syst Res 2002;63:9–26.

[17] Khuntia SR, Panda S. Simulation study for automatic generation control of a multi-area power system by ANFIS approach. Appl Soft Comput 2012;12:333–41.

[18] Ali ES, Abd-Elazim SM. Bacteria foraging optimization algorithm based load frequency controller for interconnected power system. Int J Electr Power Energy Syst 2011;33:633–8.

[19] Panda Sidhartha, Yegireddy Narendra Kumar. Automatic generation control of multi-area power system using multi-objective non-dominated sorting genetic algorithm. Int J Electr Power Energy Syst 2013;53:54–63.

[20] Saikia Lalit Chandra, Sahu Shashi Kant. Automatic generation control of a combined cycle gas turbine plant with classical controllers using firefly algorithm. Int J Electr Power Energy Syst 2013;53:27–33.

[21] Daneshfar F, Bevrani H. Multi-objective design of load frequency control using genetic algorithms. Int J Electr Power Energy Syst 2012;42:257–63.

[22] Dong L, Zhang Y, Gao Z. A robust decentralized load frequency controller for interconnected power systems. ISA Trans 2012;51:410–9.

[23] Tan W, Zhou H. Robust analysis of decentralized load frequency control for multi-area power systems. Int J Electr Power Energy Syst 2012;43:996–1005.

[24] Senjyu T, Nakaji T, Uezato K, Funabashi T. A hybrid power system using alternative energy facilities in isolated island. IEEE Trans Energy Convers 2005;20(2):406–14.

[25] Lee Dong-Jing, Wang Li. Small-signal stability analysis of an autonomous hybrid renewable energy power generation/energy storage system part I: time-domain simulations. IEEE Trans Energy Convers 2008;23(1):311–20.

[26] Ray P, Mohanty S, Kishor N. Proportional integral controller based small signal analysis of hybrid distributed generation system. Energy Convers Manage 2011;52:1943–54.

[27] Das DC, Roy AK, Sinha N. GA based frequency controller for solar thermal-diesel-wind hybrid energy generation/energy storage system. Int J Electr Power Energy Syst 2012;43:262–79.

[28] Singh V, Mohanty S, Kishor N, Ray P. H-infinity robust load frequency control in hybrid distributed generation systems. Int J Electr Power Energy Syst 2013;46:294–305.

[29] Pandey SK, Kishor N, Mohanty SR. Frequency regulation in hybrid power system using iterative proportional–integral–derivative H_∞ controller. Electr Power Compon Syst 2014;42:132–48.